Monte Carlo Simulation of the Solvent Contribution to the Potential of Mean Force for the Phenol Adsorption on Au(210) Electrodes

R. S. Neves,[1,*] A. J. Motheo,[1] R. P. S. Fartaria,[2,3] F. M. S. S. Fernandes[3]

[1] *Laboratory of Interfacial Electrochemistry, Department of Physical Chemistry, Institute of Chemistry of São Carlos, University of São Paulo, Avenida do Trabalhador Sancarlense, CP 780, 13560-970 São Carlos-SP Brazil*

[2] *Department of Chemical and Process Engineering, University of Strathclyde, Glasgow, G1 IXJ, UK*

[3] *Molecular Simulation Group, CCMM, Department of Chemistry and Biochemistry, Faculty of Science, University of Lisboa, Campo Grande, Bloco C8, 1749-016, Lisboa Portugal*

Abstract

This paper reviews some recent canonical Monte Carlo simulations of the Au(210)/H_2O interface using a DFT force field developed by us. New results are reported on the solvent contribution to the potential of mean force (PMF) for the phenol adsorption, from a dilute aqueous solution, onto the Au(210) surface. The Monte Carlo simulations show the common features normally observed in the simulation of water in contact with metallic surfaces, where the water molecules adsorb forming bilayers. The molecules adsorbed over the *Top* gold sites form hydrogen bonds between the first and second solvent layers. The PMF calculations indicate that the phenol molecule penetrates the solvent layers with the aromatic ring in a perpendicular configuration and the oxygen atom pointing to the surface. The PMF results also suggest the existence of hydrogen bonds between the phenol molecule and the first solvent layer of the water molecules adsorbed onto the *Top* sites.

Keywords: potential of mean force, phenol adsorption, Au(210), Monte Carlo simulation.

Introduction

The adsorption of ionic species and organic molecules on electrode surfaces is of the utmost importance in the field of interfacial electrochemistry, since it affects a large variety of electrode processes. For example, adsorption is involved in the

---

* Corresponding author. E-mail address: rodrigo_santis_neves@yahoo.com.br

mechanism of charge transfer reactions at electrode surfaces [1-3], capacitance dispersion in the electrode/solution interface [4-10] and self-assembly processes [11-16]. As such, adsorption is a crucial subject for various technologic research fields, ranging from surface modification [17-19] to heterogeneous catalysis applied to fuel cells [20-22].

In the last decades, *ab initio* quantum calculations, especially those using density functional theory (DFT) [23-36], and molecular simulation techniques, namely Monte Carlo (MC) [37-45] and molecular dynamics (MD) [46-55], have become powerful tools to study molecular and ionic adsorption on metallic surfaces.

The *ab initio/DFT* calculations of the interactions between different molecules and ions with a broad variety of metallic clusters, representing different crystallographic orientations of noble metals, mainly platinum [29, 32, 35], gold [25, 31, 34-36, 56, 57], copper [24, 27, 36, 57-59] and silver [27, 36, 57, 60, 61], enable to draw a picture of the influence of the surface structure on the adsorption processes. The results of such calculations have pointed, for example, to the occurrence of preferential site adsorption and the influence of the site geometry on the orientation of adsorbed molecules. These calculations are also the basis of the development of analytical potential functions to be used in MD and MC simulations of adsorption processes, such as halides on copper [39], water on platinum [55, 62] and gold [34], and ethanol on gold [31].

MD and MC simulations have provided invaluable information on the structure of the adsorbed layers, assessing the preferential orientation of adsorbed molecules in the presence of the solvent, the preferential sites for adsorption and the changes on the interface properties in the direction normal to the surface.

For example, the MD simulations carried out by Yeh and Berkowitz [55] showed that water molecules adsorb at every top site, with a square lattice packing in a Pt(100) surface, whilst in the case of the Pt(111) surface, the molecules still adsorb at top sites, but form rings of six and five molecules around an unoccupied site. This study also showed that the introduction of surface corrugation remarkably affects the adsorbed layer structure and, in a minor degree, the distribution of water molecules in the direction normal to the surface.

More recently, the MC simulations of water adsorption on the Au(210) surface, carried out by Neves et al. [38], have also shown that the molecules adsorb preferentially on top sites, but the high surface corrugation degree and heterogeneity strong influences the orientation of water molecules adsorbed on different sites. The results also indicate that molecules in the first adsorbed layer, with the molecular plane perpendicular to the surface, form hydrogen bonds between the first and second layers.

Besides the structural and dynamical properties from these simulation studies, it is important to understand the driving forces involved in the adsorption process, particularly the contribution of the solvent structure to them. To this end, potential of mean force calculations (PMF) are able to assess the solvent contribution to the total variation of the adsorption free energy, considering the influence of the surface sites involved and the adsorbing molecules orientation [37, 39, 51, 63]. The PMF may also provide additional information, especially in the cases of 2D transitions in the adsorbed layer or reorientation of the adsorbed

molecules. Indeed, the understanding of the relaxations that take place during the processes is invaluable to probe dissipative phenomena at the interface [4-7].

In the case of phenol adsorption on noble metal electrodes, electrochemical studies [64] have shown that, at potential of zero charge (pzc), the phenol molecules adsorb parallel to the surface on polycrystalline gold. However, for potentials greater than pzc, the adsorbed molecules change to a perpendicular orientation, with the oxygen atom pointing to the surface. Moreover, studies of phenol adsorption on platinum [65] have shown that the same behaviour is observed for adsorption from dilute solutions, but when it takes place from concentrated solutions, the perpendicular orientation is always the preferred one.

In a previous work we have realized PMF calculations for the phenol adsorption on a flat gold electrode [37], which show that the molecule firstly adsorbs almost perpendicular to the surface and then changes its orientation to the parallel one observed experimentally. The results have also indicated that this behaviour is clearly associated to the strong repulsion between the water layer adsorbed on the surface and the adsorbing phenol molecule, when it approaches the surface in the parallel orientation. Nonetheless, since this study used a flat surface, the influence of the surface corrugation on the preferential adsorption and on the local properties of the solvent layer has not been assessed.

In this context, the objective of the present work is to calculate, by canonical MC simulations, the solvent contribution to the PMF for the adsorption of phenol, from a dilute aqueous solution, now on a corrugated Au(210) electrode, over different surface sites and molecular orientations under conditions similar to pzc, from a DFT force field recently proposed by us [34]. The Au(210) surface is a suitable choice, since it is experimentally accessible as a single crystal surface that does not undergoes potential induced surface reconstruction, and has electrochemical characteristics resembling those of gold polycrystalline surfaces due to its high heterogeneity [66, 67].

Section 2 outlines MC and PMF computational details as well as the interaction potentials used in the simulations. Section 3 reviews some previous results related to the MC simulations of the Au(210)/H_2O interface, and reports the new calculations of the solvent contribution to the PMF for the phenol adsorption on the Au(210) surface. Finally, section 4 presents the concluding remarks.

Models and methods

Monte Carlo simulations of the Au(210)/H_2O interface

The canonical MC simulations were carried out on a system composed by 1000 molecules of water encapsulated by two Au(21 0) surfaces in the z direction. The simulation box was of rectangular shape, with 22.43 Å, 26.40 Å and 50.47 Å in the x, y and z directions, respectively. Standard periodic boundary conditions (PBC) were applied to the simulation box on the x and y directions and the dimensions of the box in these directions were chosen in order to ensure the periodicity of the crystallographic surface under the PBC. The total simulation box volume was chosen in order to reproduce the density of water at temperature and pressure of 298.25 K and 1 bar, respectively.

Equilibration runs of 5,000 MC cycles were performed prior to the production runs consisting of 25,000 MC cycles. Each cycle consisted of random translations and rotations applied to each water molecule of the system, with an acceptance rate of ~50%. The simulations were carried out using the time saving energy repository algorithm [68].

Ewald's sum method, adapted to a two dimensional periodic system [69, 70], was used to calculate the long range corrections for the electrostatic component of the interactions in the liquid phase.

Calculation of the solvent contribution to the PMF for the phenol adsorption

The PMF acting on the phenol molecule at distance z from the Au(210) surface is defined as the reversible work necessary to approach the molecule, in a determined orientation inside the solvent, from a distance z_0, where the influence of the electrode can be neglected, to a nearer distance z. Thus, the PMF is the Helmohltz free energy change taking into account the presence of the solvent.

The total free energy change (ΔA) has two contributions: one due to the solvent (ΔA_S) and other due to the interaction of the adsorbing molecule and the electrode surface. The solvent contribution can be calculated by the free energy perturbation (FEP) method [71-73], whose general equation can be written as:

$$\delta A_S^i(z_i \rightarrow z_i + \delta z) = kT \ln \langle exp \left[\frac{U(z_i + \delta z) - U(z_i)}{kT} \right] \rangle_{z_i} \qquad (1)$$

where $U(z_i)$ is the potential energy of a configuration of the reference system, $U(z_i + \delta z)$ is the potential energy of a configuration of the perturbed system, k is the Boltzmann constant and T the absolute temperature. In eq. 1, the brackets represent the ensemble average over an assembly of configurations, generated for the reference system by random translations and rotations of the water molecules composing the system, but keeping the adsorbing molecule at the distance z_i (measured from its mass centre to the electrode) and at a fixed orientation. In this stage of the calculations, only the water-water, water-phenol and water-electrode interactions are accounted for. The assembly of configurations for the perturbed system are the same as the preceding ones concerning the water molecules, but with the phenol molecule at the same orientation in the new fixed distance ($z_i + \delta z_i$), where δz_i is a small displacement applied to the phenol molecule in order to generate the perturbed system. The reference and perturbed states are different only in what concerns the phenol molecule position and they can be identified by the coordinate z of the centre of mass of the adsorbing molecule.

Under these conditions, the term $U(z_i + \delta z_i)-U(z_i)$ in eq. 1 is the difference between the phenol – water interaction potential energies in the two states, since the solvent-solvent and solvent-electrode interaction potential energies are the same for the reference and perturbed systems.

To ensure a consistent convergence of the calculated PMF, the difference between the energies for the reference and the perturbed states must be considerably smaller than kT. For calculations effects, it means that the distance $z-z_0$ should be divided into a number of windows (N_w), each one characterized by

the z_i of eq. 1. The solvent contribution to the potential of mean force, acting on the phenol molecule at distance z, is calculated by the sum of eq. 1 over the N_w windows:

$$\Delta A_S(z_0 \to z) = \sum_{i=1}^{N_w} \delta A_S^i \qquad (2)$$

For each window, the ensembles of states were generated by canonical MC simulations under the same conditions presented in section 2.1, with the addition of one single phenol molecule. Equilibration runs of 15,000 MC cycles followed by production runs of 10,000 cycles were performed for each window. The first window was chosen at a distance $z_0 = 13.5$ Å from the Au(210) surface and the following windows were located at successive displacements of 0.22 Å toward the surface. The selected perturbation distance, δz_i, was 0.1 Å and a double-wide sampling was used [72]. In order to improve the relaxation of the solvent surrounding the adsorbing phenol molecule, during the production runs the phenol molecule was allowed to move in the directions parallel to the surface (x and y), however keeping the orientation fixed.

The calculations were carried out considering two molecular orientations for the phenol adsorption on three surface sites: Top*(T)*, *Hollow 1 (H1)* and *Hollow 2 (H2)*, related, respectively, to the gold atoms of the first, second, and third and fourth surface layers (see Fig.1) . The selected orientations were: *i)* O1: aromatic ring parallel to the surface; *ii)* O2: aromatic ring perpendicular to the surface, with the oxygen atom pointing to the surface. These are the most interesting geometries considering the structural properties of the molecules and the previous experimental and theoretical works on phenol adsorption [37, 64].

Interaction force fields

The interactions between the components of the liquid phase were described by the 12-6 Lennard – Jones potentials between the sites of each molecule, submitted to a cut off radius of 8 Å, combined with Coulombic interactions related to the partial charges at each site and Ewald's sum for their long range corrections.
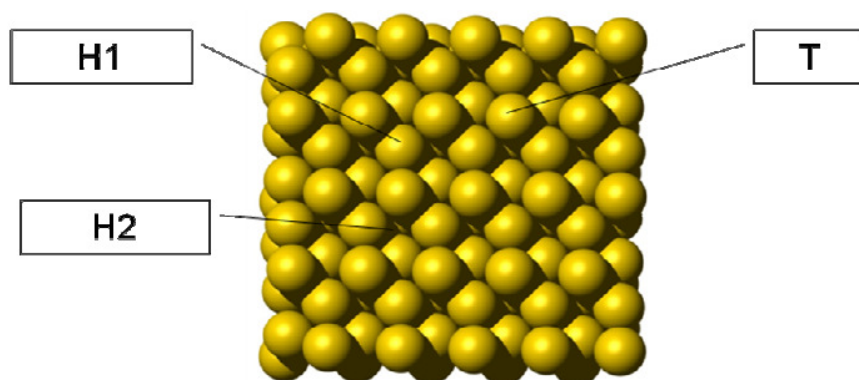

Figure 1. Section of an Au(210) surface used for the simulations. The sites T, H1 and H2 are indicated by the arrows.

Table 1. Interaction parameters for the atoms on the liquid phase.

	ε / kJ mol^{-1}	σ / Å	q / e
Water – TIP4P			
O	0.649	3.15	0
H	0	0	0.5200
e	0	0	-1.0400
Phenol			
$H(O)$	0	0	0.4400
O	0.650	3.07	-0.6400
C_1	0.294	3.55	0.5400
$C_{2,6}$	0.294	3.55	-0.4125
$C_{3,5}$	0.294	3.55	-0.0300
C_4	0.294	3.55	-0.3000
$H_{1,5}$	0.126	2.42	0.2000
$H_{2,4}$	0.126	2.42	0.1430
H_3	0.126	2.42	0.1590

In the case of the water molecules, the TIP4P [74] model was used. This model is composed by 4 interaction sites, three of them corresponding to the atoms of the water molecules and one related to the electronic charge density due to oxygen electronic pair, which is located 0.15 Å apart from the oxygen, between the two hydrogen atoms. The phenol interaction parameters and geometry were those proposed by Mooney et al. [75], with the internal degrees of freedom constrained to the minimal energy molecular geometry. All the potential parameters are presented in Table 1 and the indexes for the phenol atoms can be seen in Fig. 2.
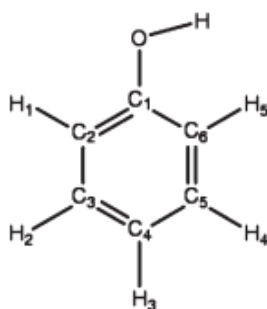
Figure 2. Representation of the phenol molecule with the indexes used in Table 1.

The interactions between the water molecules and the Au(210) were modelled by the DFT force field recently proposed by us, whose full details are described elsewhere [34], submitted to a cut off radius of 25 Å. As this force field is somewhat elaborated we recall here its main components. The general form of the potential is:

$$U_{H_2O-Au(210)}(x,y,Z) = U_T(Z) + U_{H_1}(Z)A(x,y) + U_{H_2}(Z)B(x,y);$$
$$Z \equiv \{z_0, z_{Ha}, z_{Hb}\}$$

(3)

were U_T is the interaction energy for the water molecule with the TOP site of the Au(210) surface, which is taken as the reference energy, and U_{H1} and U_{H2} are the energetic contributions, relatively to the *TOP* site, of the water molecule interaction with the sites *H1* and *H2*, respectively. These functions depend only on the distances (z_O, z_{Ha} and z_{Hb}) between each atom of the water molecules and the plane defined by the first atomic layer of the surface:

$$U_{site}(Z) = U_{O-Au}(z_O) + U_{Ha-Au}(z_{Ha}) + U_{Hb-Au}(z_{Hb}) \tag{4}$$

The structural periodicity of the surface is introduced in the force field through the functions *A(x,y)* and *B(x,y)*:

$$A(x,y) = f(x)\sin\left(\frac{1.74 + b \cdot y}{2}\right)^8 + [1 - f(x)]\cos\left(\frac{1.74 + b \cdot y}{2}\right)^8 \tag{5}$$

$$B(x,y) = f(x)\cos\left(\frac{1.40 + b \cdot y}{2}\right)^8 + [1 - f(x)]\sin\left(\frac{1.40 + b \cdot y}{2}\right)^8 \tag{6}$$

where *x* and *y* are the co-ordinates of the centre of mass of the water molecule parallel to the metallic surface and perpendicular to the *z* direction. The functions *f(x)* and *b* depend on the parameter of the gold cell (a = 4.0786 Å):

$$f(x) = \sin\left(\frac{\pi x}{a}\right)^2 \tag{7}$$

$$b = \frac{2\pi}{a\sqrt{5}} \tag{8}$$

When the centre of mass of the water molecule is over the site *T*, both functions *A(x,y)* and *B(x,y)* are equal to zero and eq. 3 reduces to U_T. If the centre of mass of the molecule is over site *H1*, *B(x,y)* is zero and *A(x,y)* = 1, and the interaction energy is $U_T + U_{H1}$. Finally, when the centre of mass is over the site *H2* *A(x,y)* = 0 and *B(x,y)* = 1, and the interaction energy is $U_T + U_{H2}$. As the x and y co-ordinates are measured from a site *T*, any of these sites can be used since the surface is periodic.

The application of eq. 3 requires the knowledge of the functions U_T, U_{H1} and U_{H2}. They are written (see eq. 4) as the sum of the interactions between each water atom and the surface:

$$U_{O-Au}(z_O) = c_0 \exp(c_1 z_O) - c_2 \exp(c_3 z_O) - c_4 \exp(c_5 z_O) \tag{9}$$

$$U_{H-Au}(z_H) = c_6 \exp(c_7 z_O) - c_8 \exp(c_9 z_O) \tag{10}$$

The coefficients of eqs. (9) and (10) are given in Table 2.

Table 2. Coefficients of the equations 8 and 9 for the different surface sites.

Coefficient	T	H1	H2
C_0 / kJ mol^{-1}	4.774×10^6	4136.72	7642.4
C_1 / Å^{-1}	-5.12	-1.67	-1.66
C_2 / kJ mol^{-1}	4015.23	4.709×10^6	4.773×10^6
C_3 / Å^{-1}	-1.69	-5.12	-5.12
C_4 / kJ mol^{-1}	0	341.73	3214.1
C_5 / Å^{-1}	0	-1.11	-1.50
C_6 / kJ mol^{-1}	43994.8	5900	3888.21
C_7 / Å^{-1}	-3.48	-3.24	-3.09
C_8 / kJ mol^{-1}	3.33798	46500	47771.9
C_9 / Å^{-1}	-0.16	-3.44	-3.45
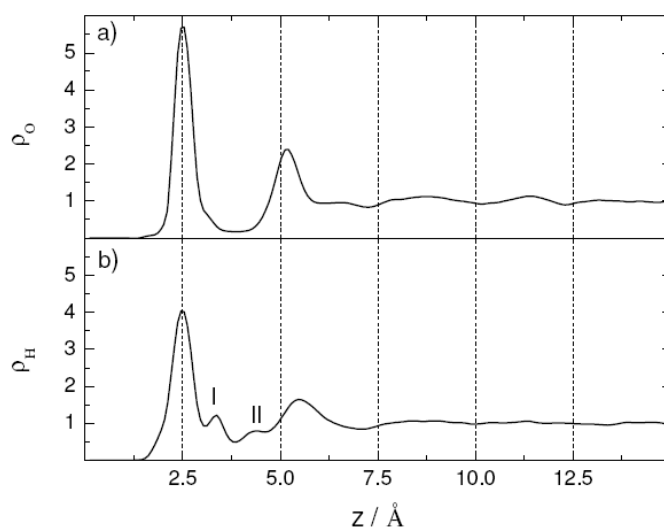
Figure 3. Normalized density profiles for water molecules at the interface. a) oxygen atoms, b) hydrogen atoms.

Results and discussions
Au(210)/H$_2$O interface

The structural characteristics of the interface are of utmost importance for the proper interpretation of the PMF results. As such, we review here the main aspects of our previous MC simulations which have been reported elsewhere [38].

The dependence of the normalized density profiles of the water molecule atoms on the distance from the surface, calculated as the average of the values for both gold surfaces in the simulation box, are presented in Fig. 3. They show two well defined water layers on the gold surface.
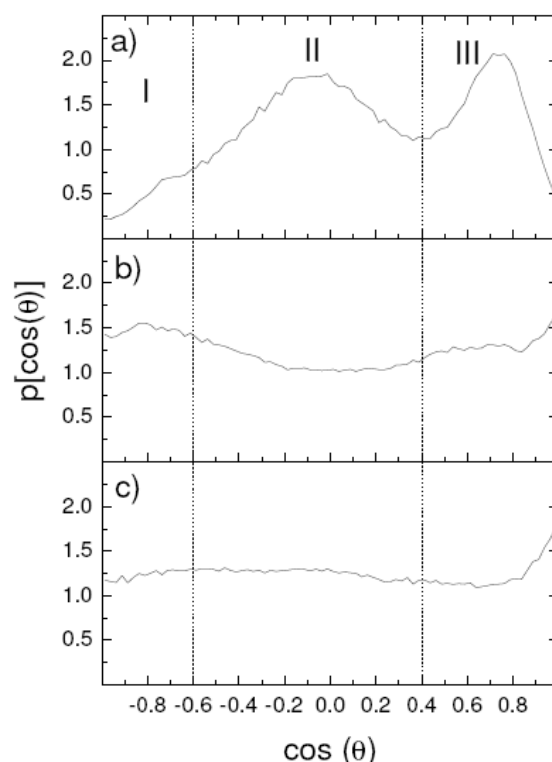
Figure 4. Distribution of the cosine of the angle between the dipole moment vector of the water molecules and the axis normal to the surface for three solvent lamina parallel to the surface. a) First lamina (between 0 and 4 Å), b) second solvent lamina (between 4 and 8 Å), c) region with weak influence from the metal.

The first layer is at the region between ~1.2 and 3.8 Å. The two most intense peaks, for the O (Fig. 3a) and H (Fig. 3b) atoms are at nearly the same distance from the surface ($\approx$ 2.5 Å), meaning that most of the water molecules in this region are adsorbed, on average, with the molecular plane parallel to surface. The sharpness of the peaks indicates that the molecules in the first solvent layer are adsorbed in well defined positions and orientations. Yet, Fig. 3b shows a small peak at ~ 3.3 Å (peak I), which also suggests that some water molecules have one or both hydrogen atoms pointing away from the surface, as observed in other simulations of water in contact with different metallic surfaces [55].

The second solvent layer extends from ~ 3.8 to ~ 6.9 Å. The peaks in this region are less intense and broader than those of the first layer, meaning that the second layer is more diffuse and less organized than the first. The molecules in this region present a higher degree of mobility and a broader distribution of the relative molecular orientations. The structure of the second layer has similar overall orientations to the first layer, but not in the same proportion, as indicated by the displacement of the more intense peak in Fig. 3b, for the hydrogen atoms distribution, when compared with the peak corresponding to the oxygen atoms (Fig. 3a). As for the small peak in Fig 3b, at ~ 4.3 Å (peak II), it suggests that some of the hydrogen atoms in the second layer are pointing towards the first layer. The relation between the peaks I and II, and the ones for oxygen was discussed elsewhere [38]. They indicate the existence of hydrogen bonds between the second and first solvent layers, what is also observed for water adsorbed over other metals.

For distances greater than 12.5 Å from the surface, the density profiles in Fig. 3 converge approximately to 1, that is, the influence of the surface can be neglected at those distances.

Additional structural information about the two solvent layers can be obtained from the distributions of the dipole moment (v_{dm}) and H–H (v_{H-H}) vectors. These distributions were calculated as a function of the cosines of the angles between those vectors and the axis normal to the surface, for three solvent laminae, each with thickness of 4 Å measured from the metallic surface. This dimension is, approximately, the observed one for the first and second water adsorbed layers.

The v_{dm} distributions are shown in Fig. 4. In the first solvent lamina, between 0 and 4 Å (Fig. 4a), the major part of the dipole moments are distributed approximately parallel to the surface, as indicated by the broad peak at ~cos (θ) = 0 (region II). In the same figure, another peak is observed in region III, at ~ cos (θ) = 0.75, corresponding to those molecules adsorbed with molecular plane approximately perpendicular to the surface. It is interesting to point out that, in this configuration, the hydrogen atom pointing towards the electrode is at ~3.4 Å from the surface, in agreement with the results for the hydrogen density profile (Fig. 3b – peak I). As stressed in our previous paper [38], these structural properties resembles the water bilayers formed in the adsorption of water molecules on closed packed noble metal surfaces [76, 77], despite the fact that the Au(210) presents a more heterogeneous structure.

In the solvent lamina between 4 and 8 Å (Fig. 4b), a very weak v_{dm} preferential orientation tendency is observed around cos (θ) = -0.75 Å (region I), suggesting that the hydrogen atoms are pointing towards the bulk liquid phase, in agreement with the density profiles of Fig. 3. It is also possible to see a weak wave at cos (θ) = - 0.6 (region I), which is related to peak II of Fig. 3b and is an additional evidence of the hydrogen bonds referred to above.

In the case of the solvent lamina located between 8 and 12 Å (Fig. 4c), no appreciable v_{dm} preferential orientation is observed and the liquid structure approaches the bulk behaviour.

The distributions of the v_{H-H} vectors are presented in Fig. 5. They support the conclusions presented above. In the first solvent lamina (Fig. 5a), the major part of the v_{H-H} is nearly parallel to the surface (region II, peak at ~ cos (Φ) = 0), whilst the small peaks in regions I and III indicate the presence of some molecules adsorbed with the molecular plane perpendicular to the surface. Both observations are in clear agreement with v_{dm} distribution (Fig. 4a).

In the case of the second solvent lamina, between 4 and 8 Å (Fig. 5b), a weaker v_{H-H} preferential orientation tendency is observed as for the v_{dm} distribution in the same lamina (Fig. 4b), thus corroborating the formation of hydrogen bonds between the different solvent layers.

For the last solvent lamina, between 8 and 12 Å (Fig. 5c) no specific tendency is observed and the solvent structure resembles that of the bulk.
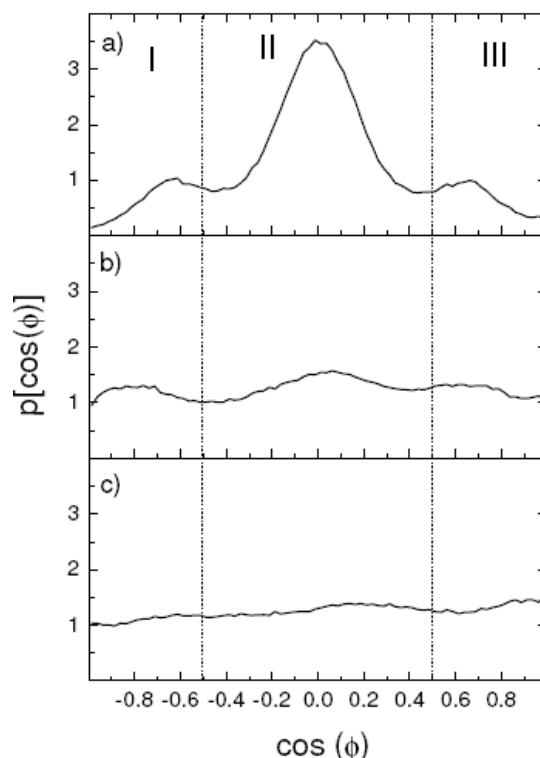
Figure 5. Distribution of the cosine of the angle between the H-H vector of the water molecules and the axis normal to the surface for three solvent lamina parallel to the surface. a) First lamina (between 0 and 4 Å), b) second solvent lamina (between 4 and 8 Å), c) region with weak influence from the metal.

To proper understand the PMF calculations of the solvent contribution to the phenol adsorption, it is necessary to assess not only the mean structural properties of the water layer over the surface as a whole, but also the adsorbed water configuration over the different surface sites. Our previous results [38] have essentially shown that the water molecules of the first adsorbed layer adopt a configuration very close to the so called ice like structure, forming irregular hexagonal structures with a molecule in the centre. On average, the molecules adsorb preferentially over *T* sites, followed by the *H1* sites, with a low water density over the *H2* sites. An interesting feature is that the water molecules in the first solvent layer, with the molecular plane nearly perpendicular to the surface, adsorb preferentially on the *T* sites. The hexagonal structures in the first water layer are represented in Fig. 6. The oxygen surface density distribution, in Fig. 7, shows the higher densities over the *T* sites, followed be the *H1* ones. Fig. 8, presents the surface density of the hydrogen atoms in the region of the first solvent layer related to the peak I of Fig. 3b, which form hydrogen bonds with the second layer. It indicates that the hydrogen density is significantly higher over the *T* sites.
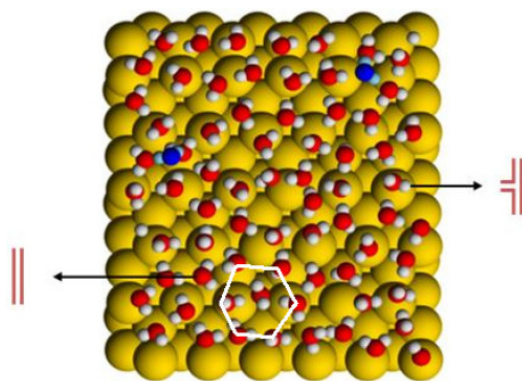
Figure 6. Snapshot of the water molecules adsorbed on the Au(210) surface. The darkest oxygen atoms are of water molecules interacting with the first solvent layer via hydrogen bonds. Hexagonal centred structure is highlighted.
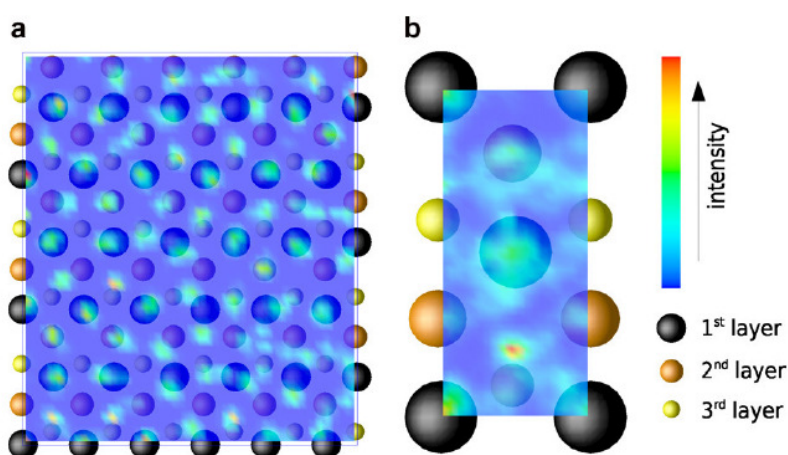

Figure 7. Oxygen surface density distribution in the first solvent layer: (a) total surface and (b) surface unit cell (ref [38], with Elsevier's permission).
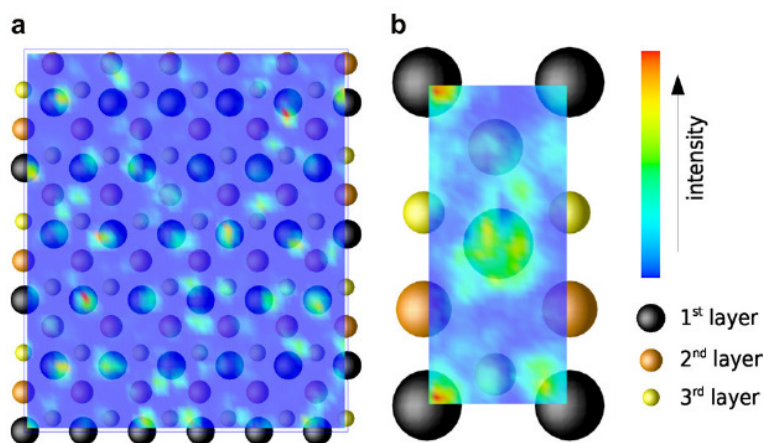

Figure 8. Hydrogen surface density distribution of the hydrogen atoms in the first solvent layer, which form hydrogen bonds with the second solvent layer: (a) total surface and (b) surface unit cell (from ref [38], with Elsevier's permission).

Solvent contribution to the PMF for the phenol adsorption

The contribution of the solvent to the total free energy change associated to the adsorption of phenol from a dilute aqueous solution on the sites *T*, *H1* and *H2* of the Au(210) surface, for the orientations *O*1 and *O*2, are presented in Fig. 9.
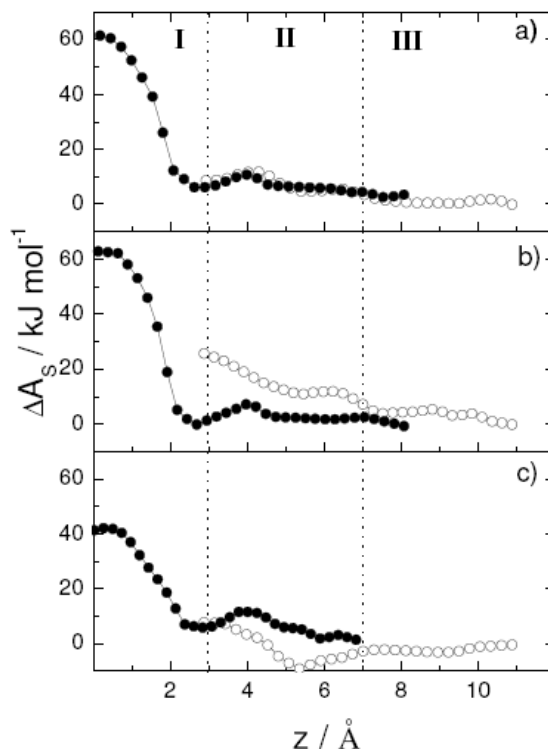

Figure 9. Solvent contribution to the PMF for the phenol adsorption onto different sites of the Au(210) surface: a) site *H2*, b) site *H1*, c) site *T*. (●) orientation *O1*, parallel to the surface; (○) orientation *O2*, perpendicular to the surface.

When the phenol molecule approaches the surface with the *O1* orientation, where the aromatic ring is parallel to the surface, a strong repulsion between the phenol molecule and the first water adsorbed layer is verified for all the studied sites. This repulsion is represented by the high positive values of $\triangle A_S$ when the distance of the centre of mass of the phenol molecule (CM_{Ph}) from the surface is less than 3 Å (region **I**) and comes from the "compression" of the solvent layer by the aromatic ring, which naturally blocks the phenol adsorption directly at the surface. In the region between 3 and 5 Å (region II), where the phenol molecule interacts with the second solvent layer, a less intense repulsion is observed, since the structure of this layer is less organized, as indicated by the above MC simulations. Similar results were observed in our previous study with a non structured (flat) gold surface [37], suggesting that this repulsion is relatively uninfluenced by the surface structure, but uniquely by the interactions between the phenol molecule and the first solvent layer, independent of the local structure of the layer.

When the molecule approaches the surface in the *O2* orientation, however, distinct behaviours are observed for the different sites. In the case of the sites *H2* (Fig 9a) and *H1* (Fig. 9b), the solvent contribution when the CM_{Ph} is around 5 Å from the surface (region II), is about 10 kJ mol^{-1} for both the sites. It is worth to

remember that if the phenol molecule approaches the surface in the O2 orientation, perpendicular to the electrode, when the CM_{Ph} is at 5 Å from the surface, the OH group is well inside the first solvent layer, at ≈ 2.2 Å. In this situation, the solvent contribution to the total free energy of adsorption is still positive hindering the phenol adsorption. Yet, its value is considerably less than the one for the O1 orientation near to the electrode (≈ 60 kJ mol^{-1}), indicating that, concerning the solvent contribution, the orientation O2 favours for the phenol adsorption on sites *H1* and *H2*. Again, the same qualitative tendency was seen in our previous study with a non structured gold surface [37].

As for the site *T* (Fig. 9c), the solvent contribution is negative (≈ -10 kJ mol^{-1}) when the CM_{Ph} is at ~ 5 Å from the surface. The negative value suggests an attraction between the phenol molecule and the first solvent layer over the site *T*. This is presumably associated to the formation of hydrogen bonds between the phenol and the water molecules on sites *T*, which are adsorbed in a suitable geometry for that, as noted in section 3.1. This result indicates that when the phenol molecule approaches the surface in a perpendicular orientation, the solvent contribution to the PMF is strongly affected by the local structure of the first solvent layer, which, in region II, becomes negative for the *T* sites.

Electrochemical studies [64] and our previous MC simulations [37] have demonstrated that the final orientation of the phenol molecule adsorbed on a gold surface is the *O1*, parallel to the electrode. However, our previous PMF calculations with a flat gold surface [37] and the present results indicate that despite the final orientation, the phenol molecule should penetrate the solvent layers with the aromatic ring perpendicular and the oxygen atom pointing to the surface (orientation *O2*).

The present results support previous experimental and simulation results which show that, at the pzc, the phenol molecules, from a dilute aqueous solution, adsorb firstly in the *O2* orientation and then go through a smooth transition to the parallel configuration (*O1*). They also do not contradict the experimental observations that phenol adsorbs on noble metals, from concentrated solutions, perpendicular to the surface and does not undergo reorientation [65] , even at pzc. This presumably occurs due to the high coverage degree of the surface by perpendicular adsorbed phenol molecules, which disable the reorientation process.

Nonetheless, to properly analyze such details one needs a full quantum mechanical potential to describe the interactions between phenol and gold. This is one of the perspectives for future work.

Concluding Remarks

We have reviewed canonical Monte Carlo simulations of water adsorbed on the Au(210) surface and reported new calculations of the solvent contribution to the PMF for the phenol adsorption, from a dilute aqueous solution, onto that surface. The results show that the water molecules adsorb on the Au(210) surface forming structures similar to those observed in water bilayers on close-packed noble

metal surfaces, with the molecules adsorbed over the *T* sites forming hydrogen bonds between the first and the second solvent layers.

The PMF calculations indicate that the phenol molecule penetrates the solvent layers in a perpendicular orientation with the O atom pointing to the surface. Moreover, if the phenol molecule approaches the surface over *T* sites, in this orientation, the solvent contribution to the PMF is negative when the centre of mass of the phenol molecule is at ≈ 5 Å from the surface, suggesting an attraction between the phenol and the water molecules in the first solvent layer due to hydrogen bonds.

Acknowledgements

References

1. M.P. Soriaga, J.L. Stickney, A.T. Hubbard, *J. Electroanal. Chem.* 144 (1983) 207.

2. J.H. White, M.P. Soriaga, A.T. Hubbard, *J. Electroanal. Chem.* 177 (1984) 89.

3. M.P. Soriaga, J.H. White, D. Song, V.K.F. Chia, P.O. Arrhenius, A.T. Hubbard, *Inorg. Chem.* 24 (1985) 73.

4. A.J. Motheo, A. Sadkowski, R.S. Neves, *J. Electroanal. Chem.* 430 (1997) 253.

5. A. Sadkowski, A.J. Motheo, R.S. Neves, *J. Electroanal. Chem.* 455 (1998) 107.

6   R.S. Neves, E. De Robertis, A.J. Motheo, *Electrochim. Acta* 51 (2006) 1215.

7   R.S. Neves, E. De Robertis, A.J. Motheo, *Appl. Surf. Sci.* 253 (2006) 1379.

8   G. Láng, K.E. Heusler, *J. Electroanal. Chem.* 457 (1998) 257.

9. T. Pajkossy, T. Wandlowski, D.M. Kolb, *J. Electroanal. Chem.* 414 (1996) 209.

10. T. Pajkossy, *Solid State Ionics* 94 (1997) 123.

11. F.S. Damos, R.C.S. Luz, A.A. Sabino, M.N. Eberlin, R.A. Pilli, L.T. Kubota, *J. Electroanal. Chem.* 601 (2007) 181.

12. J. Moon, T. Kang, S. Oh, S. Hong, J. Yi, *J. Colloid Interface Sci.* 298 (2006) 543.

13. L. Thomsen, B. Watts, D.V. Cotton, J.S. Quinton, P.C. Dastoor, *Surf. Interface Anal.* 37 (2005) 472.

14. H.-G. Hong, W. Park, *Electrochim. Acta* 51 (2005) 579.

15. B. Adolphi, E. Jähne, G. Busch, X. Cai, *Anal. Bioanal. Chem.* (2004).

16. F. Schreiber, *Prog. Surf. Sci.* 65 (2000) 151.

17. J.S. Quinton, L. Thomsen, P.C. Dastoor, *Surf. Interface Anal.* 25 (1997) 931.

18. A. Avranas, N. Sedlácková, E. Malasidou, *J. Colloid Interface Sci.* 285 (2005) 665.
19. Q. Wang, L. Zhong, J. Sun, J. Shen, *Chem. Mater.* 17 (2005) 3563.
20. M.S. McGovern, P. Waszczuk, A. Wieckowski, *Electrochim. Acta* 51 (2006) 1194.
21. C. Roth, N. Benker, T. Buhrmester, M. Mazurek, M. Loster, H. Fuess, D.C. Koningsberger, D.E. Ramaker, *J. Am. Chem. Soc.* 127 (2005) 14607.
22. S.A.R.K. Deshmukh, M.v.S. Annaland, J.A.M. Kuipers, *Appl. Catal. A* 289 (2005) 240.
23. Y. Morikawa, J.J. Mortensen, B. Hammer, J.K. Norskov, *Surf. Sci.* 386 (1997) 67.
24. J.R.B. Gomes, J.A.N.F. Gomes, *J. Mol. Struc. (THEOCHEM)* 463 (1999) 163.
25. A. Ignaczak, *J. Electroanal. Chem.* 480 (2000) 209.
26. Y. Widjaja, C.B. Musgrave, *Surf. Sci.* 469 (2000) 9.
27. A. Ignaczak, *J. Electroanal. Chem.* 495 (2001) 160.
28. M. Mavrikakis, J. Rempel, J. Greeley, L.B. Hansen, J.K. Norskov, *J. Chem. Phys.* 117 (2002) 6737.
29. P.R.N. de Souza, D.A.G. Aranda, J.W.N. Carneiro, C.S.B. Oliveira, O.A.C. Antunes, F.B. Passos, *Int. J. Quantum Chem.* 92 (2003) 400.
30. P. Vassilev, R.A. van Santen, M.T.M. Koper, *J. Chem. Phys.* 122 (2005) 054701.
31. R.P.S. Fartaria, F.F.M. Freitas, F.M.S.S. Fernandes, *Int. J. Quantum Chem.* 107 (2007) 2169.
32. C. Hartnig, J. Grimminger, E. Spohr, *J. Electroanal. Chem.* 607 (2007) 133.
33. D.A.R.S. Latino, R.P.S. Fartaria, F.F.M. Freitas, J. Aires-de-Souza, F.M.S.S. Fernandes, *J. Electroanal. Chem.* 624 (2008) 109.
34. R.S. Neves, A.J. Motheo, R.P.S. Fartaria, F.M.S.S. Fernandes, *J. Electroanal. Chem.* 609 (2007) 140.
35. S. Meng, E.G. Wang, S. Gao, *Phys. Rev. B* 69 (2004) 195404.
36. A. Bilic, J.R. Reimers, N.S. Hush, R.C. Hoft, M.J. Ford, *J. Chem. Theory Comput.* 2 (2006) 1093.
37. R.S. Neves, A.J. Motheo, F.M.S.S. Fernandes, R.P.S. Fartaria, *J. Braz. Chem. Soc.* 15 (2004) 224.
38. R.S. Neves, A.J. Motheo, R.P.S. Fartaria, F.M.S.S. Fernandes, *J. Electroanal. Chem.* 612 (2008) 179.
39. A. Ignaczak, J.A.N.F. Gomes, S. Romanowski, *J. Electroanal. Chem.* 450 (1998) 175.
40. D. Song, D. Forciniti, *J. Chem. Phys.* 115 (2001) 8089.
41. T. Panczyk, P. Szabelski, W. Rudzinski, *J. Phys. Chem. B* 109 (2005) 10986.
42. U. Reimer, M. Wahab, P. Schiller, H.-J. Mögel, *Langmuir* 21 (2005) 1640.
43. P. Zarzycki, P. Szabelski, R. Charmas, *Appl. Surf. Sci.* 252 (2005) 752.
44. F.M.S.S. Fernandes, R.P.S. Fartaria, D.A.R.S. Latino, F.F.M. Freitas, *Port. Electrochim. Acta* 26 (2008) 1.

45. R.P.S. Fartaria, F.F.M. Freitas, F.M.S.S. Fernandes, *J. Electroanal. Chem.* 574 (2005) 321.
46. J.N. Glosli, M.R. Philpot, *J. Chem. Phys.* 96 (1992) 6962.
47. J.N. Glosli, M.R. Philpot, *J. Chem. Phys.* 98 (1993) 9995.
48. D.A. Rose, I. Benjamin, *J. Chem. Phys.* 98 (1993) 2283.
49. M.R. Philpot, J.N. Glosli, *Chem. Phys.* 198 (1995) 53.
50. M.R. Philpot, J.N. Glosli, S.-B. Zhu, *Surf. Sci.* 335 (1995) 422.
51. E. Spohr, *Acta Chem. Scand.* 49 (1995) 189.
52. E. Spohr, *Electrochim. Acta* 44 (1999) 1697.
53. E. Spohr, *Solid State Ionics* 150 (2002) 1.
54. E. Spohr, *Electrochim. Acta* 49 (2003) 23.
55. I.C. Yeh, M.L. Berkowitz, *J. Electroanal. Chem.* 450 (1998) 313.
56. S. Franzen, *Chem. Phys. Lett.* 381 (2003) 315.
57. A. Ignaczak, J.A.N.F. Gomes, *J. Electroanal. Chem.* 420 (1997) 209.
58. Y. Zeng, J. Yi, H. Wang, G. Zhou, S. Liu, *J. Mol. Struc. (THEOCHEM)* 724 (2005) 81.
59. C.D. Taylor, R.G. Kelly, M. Neurock, *J. Electroanal. Chem.* 607 (2007) 167.
60. V.I. Avdeev, G.M. Zhidomirov, *Surf. Sci.* 492 (2001) 137.
61. F. Tielens, M. Saeyrs, E. Tourwé, G.B. Marin, A. Hubin, P. Geerlings, *J. Phys. Chem. A* 106 (2002) 1450.
62. E. Spohr, G. Tóth, K. Heinzinger, *Electrochim. Acta* 41 (1996) 2131.
63. J.A.N.F. Gomes, A. Ignaczak, *J. Mol. Struc. (THEOCHEM)* 463 (1999) 113.
64. R.O. Lezna, N.R. de Tacconi, S.A. Centeno, A.J. Arvia, *Langmuir* 7 (1991) 1241.
65. M.P. Soriaga, A.T. Hubbard, *J. Am. Chem. Soc.* 104 (1982) 3937.
66. A. Hamelin, *J. Electroanal. Chem.* 138 (1982) 395.
67. A. Hamelin, A.M. Martins, *J. Electroanal. Chem.* 407 (1996) 13.
68. R.P.S. Fartaria, R.S. Neves, P.C.R. Rodrigues, F.F.M. Freitas, F.M.S.S. Fernandes, *Comput. Phys. Commun.* 175 (2006) 116.
69. E. Spohr, *J. Chem. Phys.* 107 (1997) 6342.
70. I.-C. Yeh, M.L. Berkowitz, *J. Chem. Phys.* 111 (1999) 3155.
71. M. Mezei, D.L. Beveridge, *Annu. New York Acad. Sci.* 482 (1986) 1.
72. C.A. Reynolds, P.M. King, W.G. Richards, *Mol. Phys.* 76 (1992) 251.
73. W.F. van Gunsteren, X. Daura, A.E. Mark, *Helvetica Chim. Acta* 85 (2002) 3113.
74. W.L. Jorgensen, J. Chandrasekhar, J.D. Madura, *J. Chem. Phys.* 79 (1983) 926.
75. D.A. Mooney, F. Müller-Plathe, K. Kremer, *Chem. Phys. Lett.* 294 (1998) 135.
76. C.D. Taylor, M. Neurock, *Curr. Opin. Solid St. M.* 9 (2005) 49.
77. J.-S. Filhol, M. Neurock, *Angew. Chem. Int. Ed.* 45 (2006) 402.